UCSD

UC San Diego
Astronomy and Astrophysics

A Kp Forecast Several Days in Advance From Solar Surface Extrapolated GSM Component Fields and Heliospheric-Derived Velocity and Density

Bernard V. Jackson[#+] Matthew Bracamontes, Benjamin Pieczynski, Andrew Buffington

Department of Astronomy and Astrophysics, University of California, San Diego 9500 Gilman Drive #0424, La Jolla, CA 92093-0424, USA

#Corresponding author: bvjackson@ucsd.edu ⁺Presenter Tel: 858-442-9532

Abstract

Our University of California, San Diego (UCSD) group now provides a Kp forecast up to five days ahead of the current time with a 70% chance of an occurrence to predict geomagnetic storms from a Kp enhancement greater than 5. We provide this from first principles using a machine learning tool and a prediction of GSM magnetic field components, velocity, and density. This forecast is currently made available on the UCSD website https://ips.ucsd.edu and to the NASA Goddard Community Coordinated Modeling Center. Our automatic system operates using near-Earth spacecraft measurements and Interplanetary Scintillation (IPS) data from existing world radio sites to provide the density and velocity forecasts. Magnetic fields using Global Oscillation Network (GONG) data sets provide GSM fields at Earth extrapolated outward from the solar surface. We have known since 2018 that we were able to forecast GSM Bz fields. However, since the summer of 2024 our machine learning tool has been used to provide the high Kp correlation with geomagnetic storms in advance of our observations. Here, we show past examples and a real time forecast from our analyses.
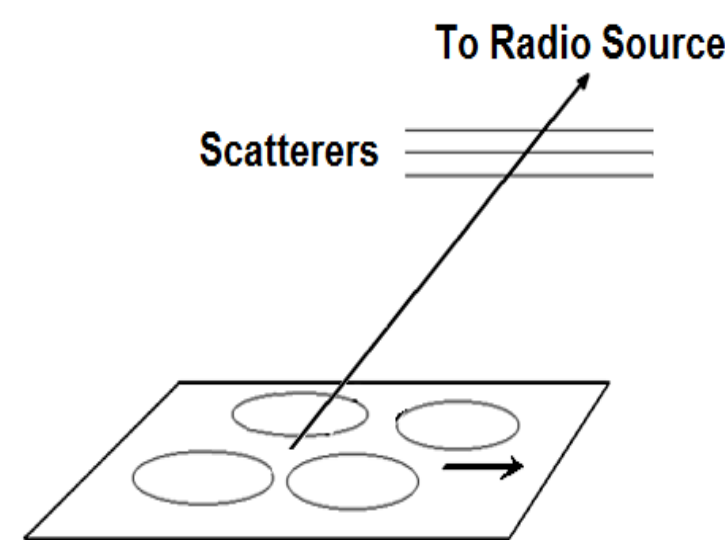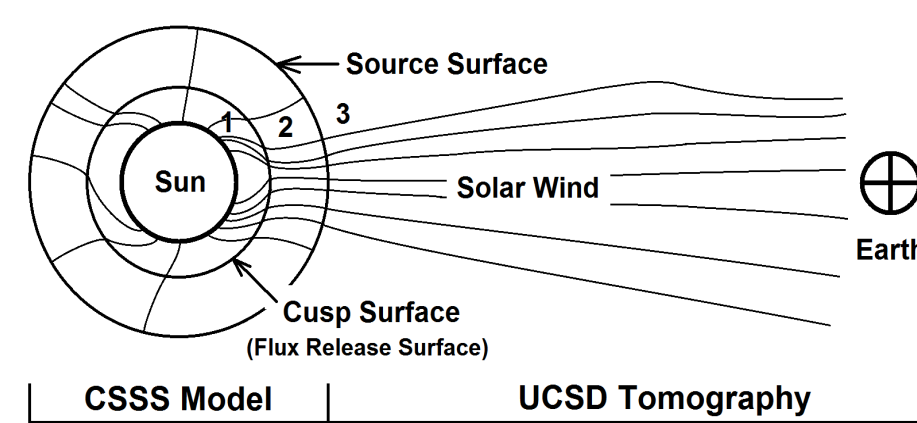
URLS: https://ips.ucsd.edu https://stereo.ucsd.edu https://stereo.ucsd.edu/PUNCH
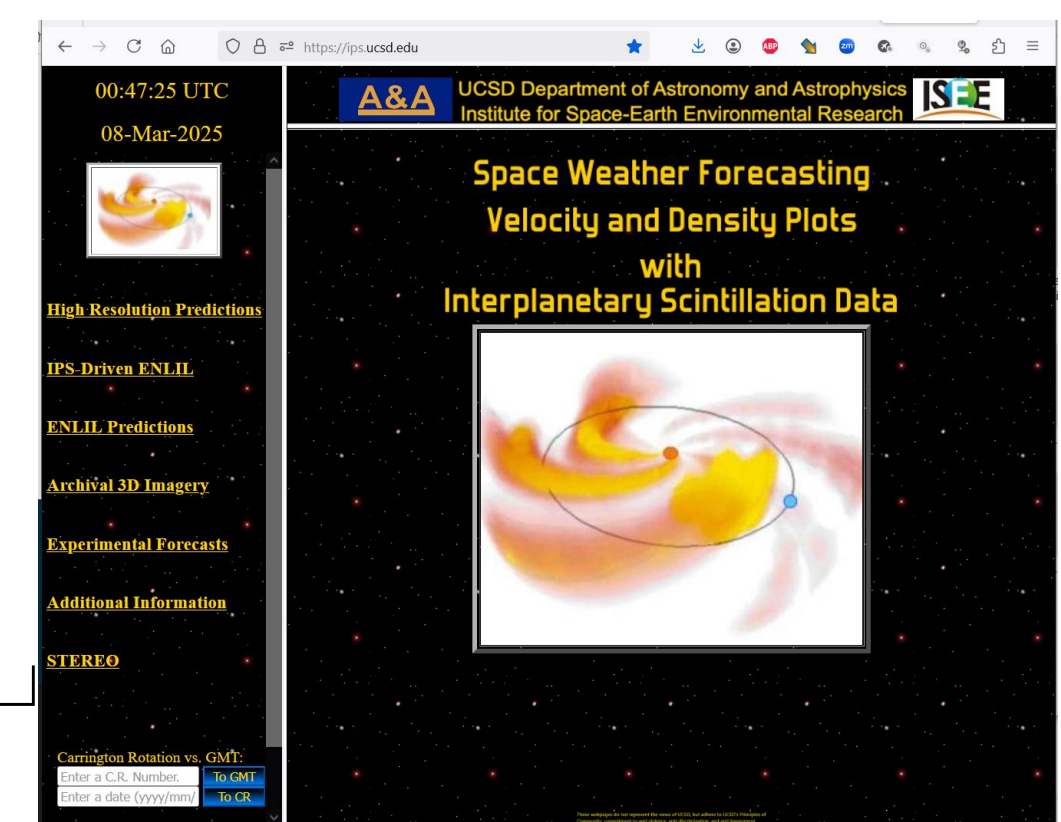
1. IPS 3-D Reconstruction Analyses

Data Source: IPS Radio Array

Point Radio Source a Proxy for Density (g-level), Velocity

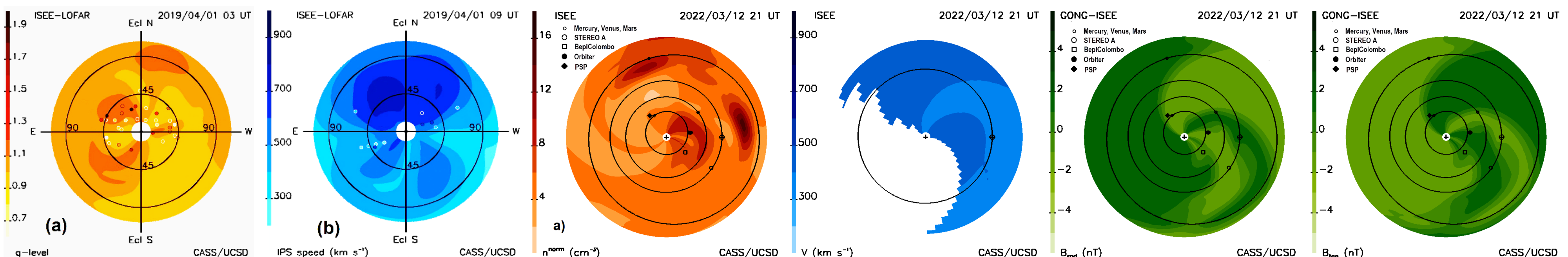**Magnetic Field Measurements (Extrapolated from GONG)**

**2000-present UCSD Webpages**
https://ips.ucsd.edu

Kinematic Model: Conserves Mass and Mass Flux, enforces radial flow

**Sample Presented Data:** (left to right) Sky Maps with fit radio sources (Scintillation or g-level, Velocity ⊥ to the LoS); Ecliptic Cuts (Density from g-level, Velocity, Magnetic Fields in RTN Bx, By from GONG data extrapolations. Skymaps are from ISEE and LOFAR analyses (Jackson *et al*., 2022); the ecliptic cuts are from Jackson *et al*., 2023, ISEE V is nonexistent at this time.)

The UCSD 3-D reconstruction analyses developed in the 1990's, and refined considerably since, provides an iterative time-dependent fit to remotely-sensed heliospheric IPS data. ISEE, Japan has long been the world standard for these data sets, but is only at one Earth longitude. These and data from other radio IPS stations around the world are sparse and use only the strongest point-like radio sources to provide observations. Thus, the physical properties of the heliosphere must be used to iterate a model that fits the data. The UCSD technique uses the outward flow of the plasma (which is mostly radial), and its known decrease in response as the solar wind moves outward to locate different structures along lines of sight (LoS). A kinematic model that conserves mass flux from one outward surface to another allows a form of outward solar wind expansion (fast structures catch up slow and compress them, slow features behind fast are rarified). The analysis then traces solar wind outward from a lower source surface in what we call a "traceback" matrix, which gives the origin of heliospheric structure on this surface at a given time. From an initial guess, a model is formally inverted on the source surface to give a best global 3-D fit to data throughout the volume (Jackson *et al*., 2003, 2020).

GONG data, refreshed every 6 hours, is used in the CSSS model (Zhao and Hoeksema, 1995) and extrapolated upward from the source surface using the IPS velocity data provide low-resolution radial and tangential magnetic fields in RTN coordinates. The Parker (1958) approximation that is used for the velocity heliographic coordinate extrapolation does not provide a normal component.
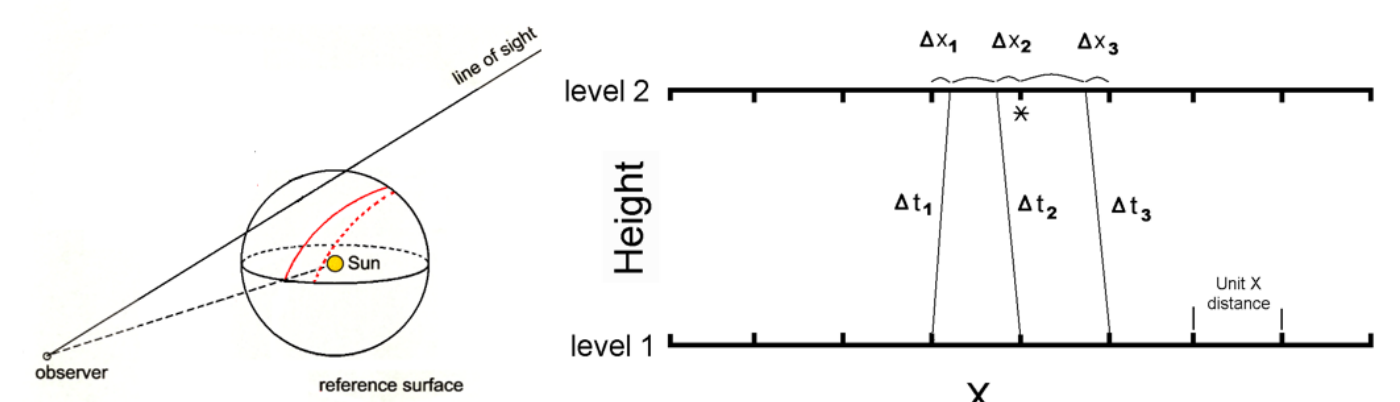
The "traceback matrix" (any solar wind model works) In the traceback matrix the location of the upper level data point (starred) is an interpolation in x of Δx2 and the unit x distance – Δx3 distance or (1 – Δx3). Similarly, the value of Δt at the starred point is interpolated by the same *spatial* distance. Each 3D traceback matrix contains a regular grid of values ΣΔx, ΣΔy, ΣΔt, ΣΔv, and ΣΔm that locates the origin of each point in the grid at each time and its change in velocity and density from the heliospheric model.
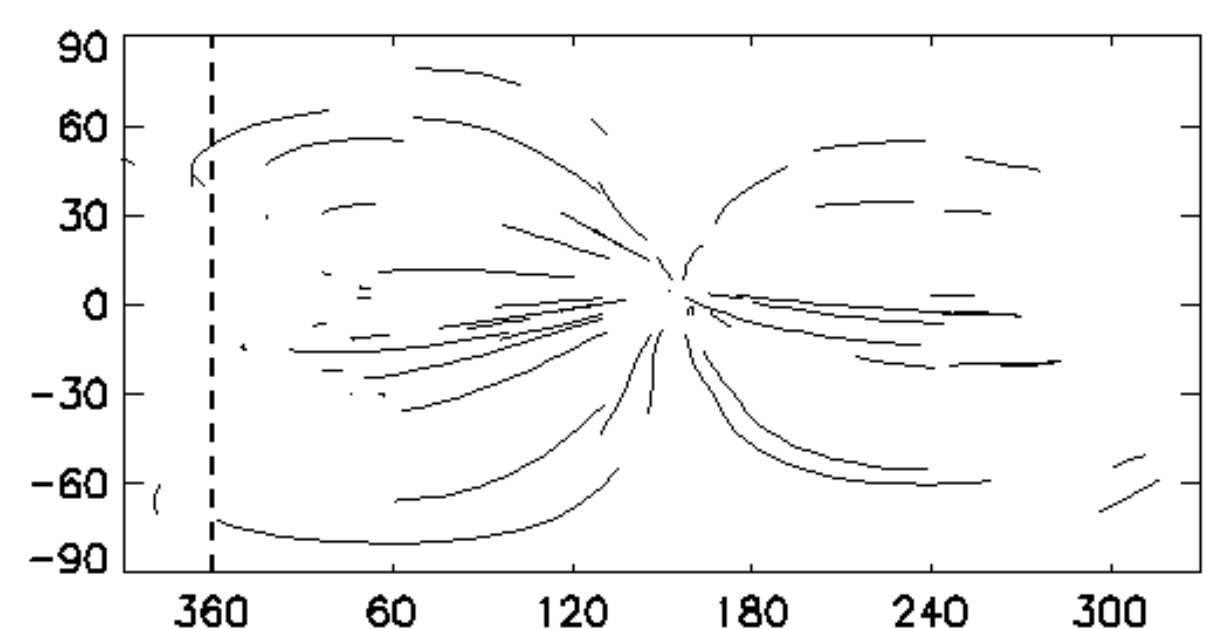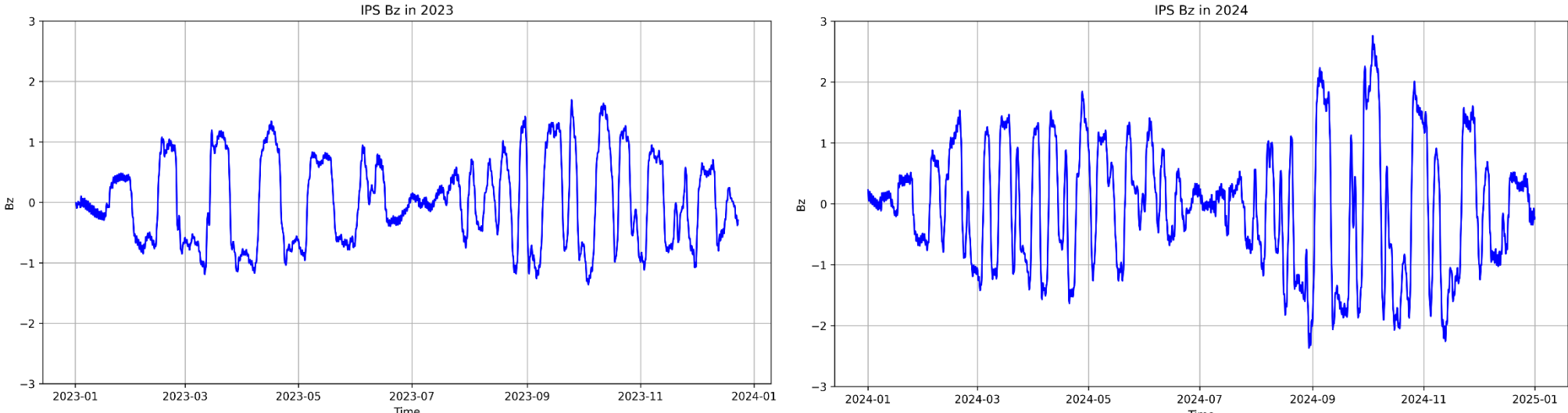

Carrington map sample of IPS LoS traced back to a source surface at 15 Rs. The source surface changes are iteratively determined by a 3-D inversion to fit the 3-D data over time.
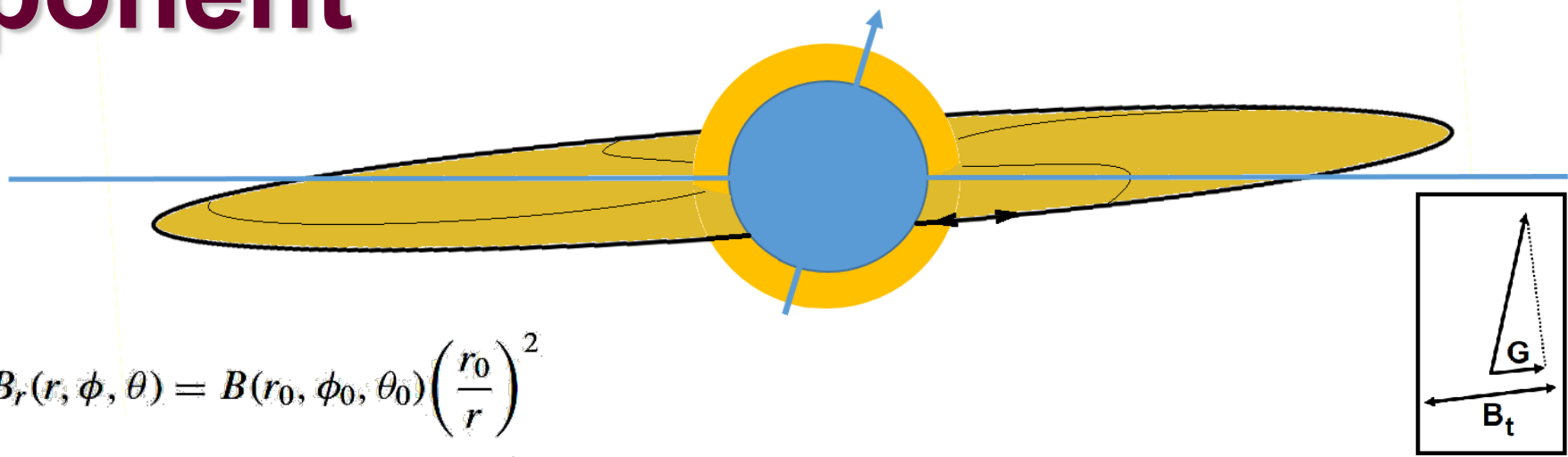
2. Determination of a GSM Bz component

The key to the UCSD Kp analysis is the determination of GSM Bz from the extrapolated RTN radial and tangential magnetic field components on a daily basis. Because of the tilt of the Earth's axis relative to the heliographic equator there is a component of the magnetic field present derived from the radial and tangential component fields that are given in the equations for the figure shown to the right. This field varies due to the toward or away from the Sun change of the radial field component on the solar surface mapped by the CSSS model.

The UCSD GSM Bz derived component and its low resolution variation over the years 2023 and 2024 are shown below. Comparisons of GSM Bz compared with ACE in real time are shown below right. The increase in geomagnetic storms near the solar equinoxes from GSM Bz relative to the heliographic equator was shown by Russell and McPherron (1973).
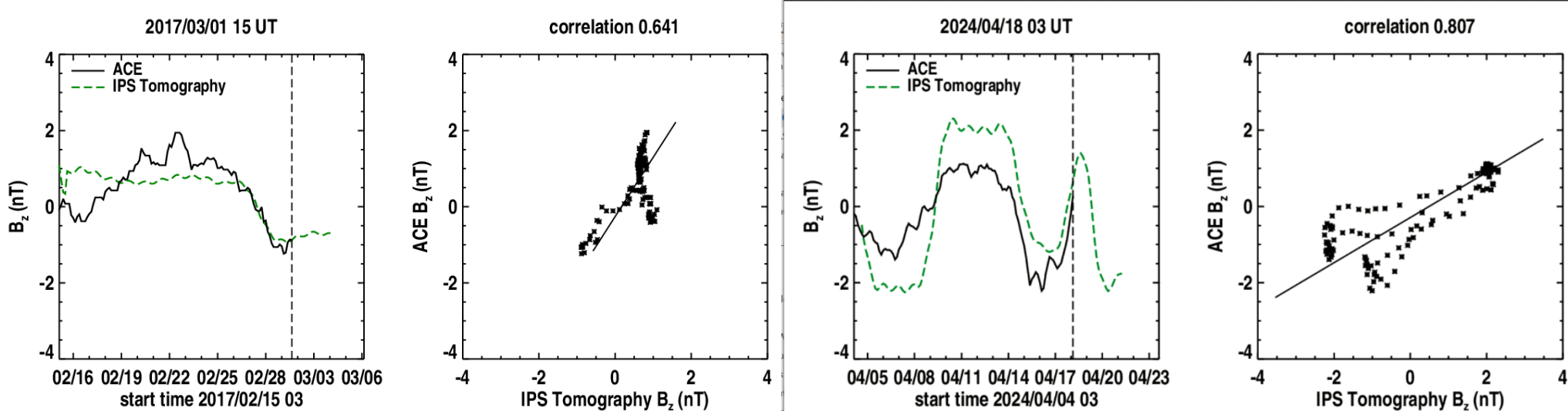
$$B_r(r, \phi, \theta) = B(r_0, \phi_0, \theta_0)\left(\frac{r_0}{r}\right)^2$$

$$B_\phi(r, \phi, \theta) = -B(r)\left(\frac{\omega r_0 \sin(\theta)}{V}\right)\left(\frac{r_0}{r}\right)$$

$$B_\theta(r, \phi, \theta) = 0$$

Earth magnetic field axis depicted at the autumnal equinox relative to the ecliptic plane and the heliographic tangential field.

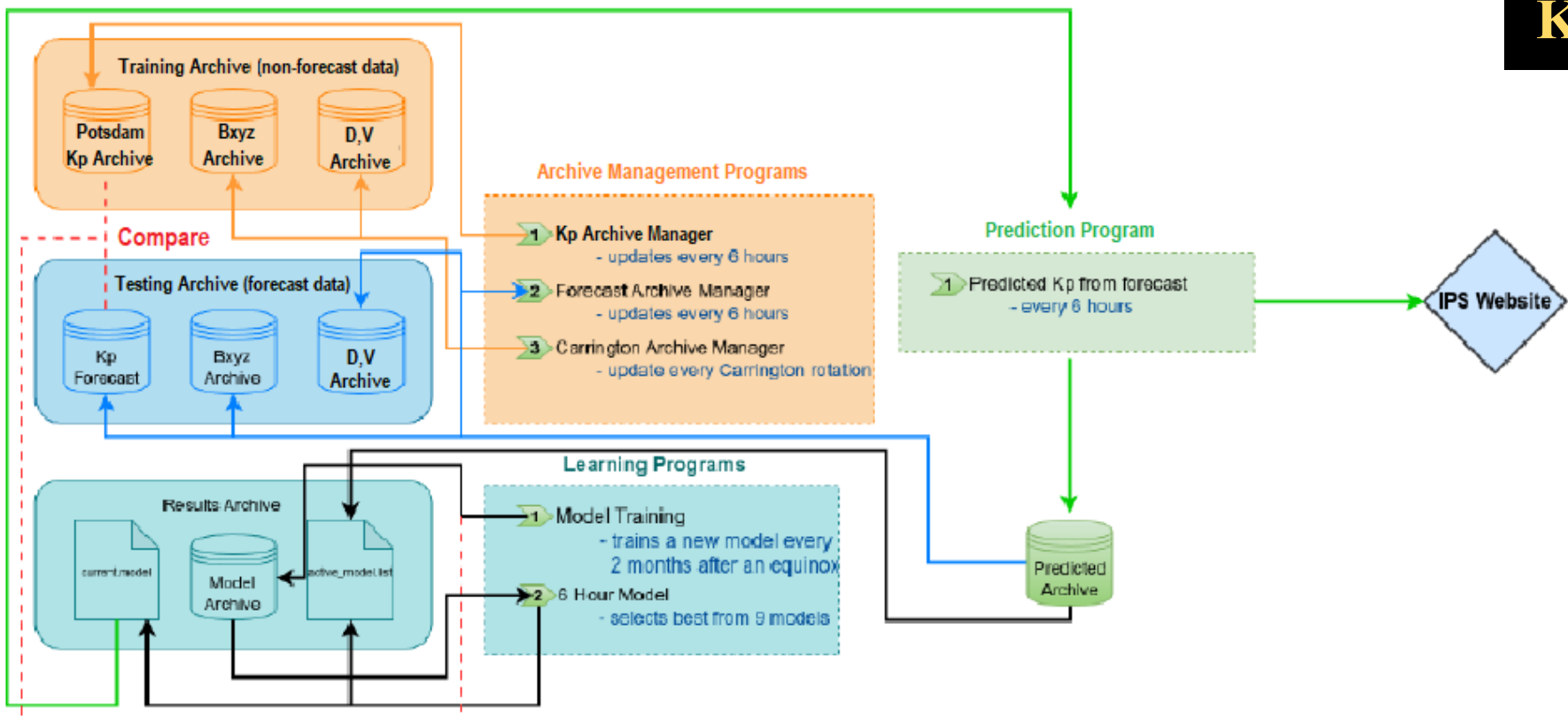**2023 and 2024 GSM Bz variations (equinoxes are 03/20 and 09/22)**

Forecasts up to 5 days ahead of GSM -Bz excursions compared to ACE measurements for two time periods with associated moderate geomagnetic storms on 2017/03/01 12UT – 2017/03/02 12UT (Kp 5), and 2024/04/20 01 UT – 2024/04/20 23 UT (Kp 7). The earlier –Bz dip on 2024/04/15 was associated with a max Kp of 5.6.
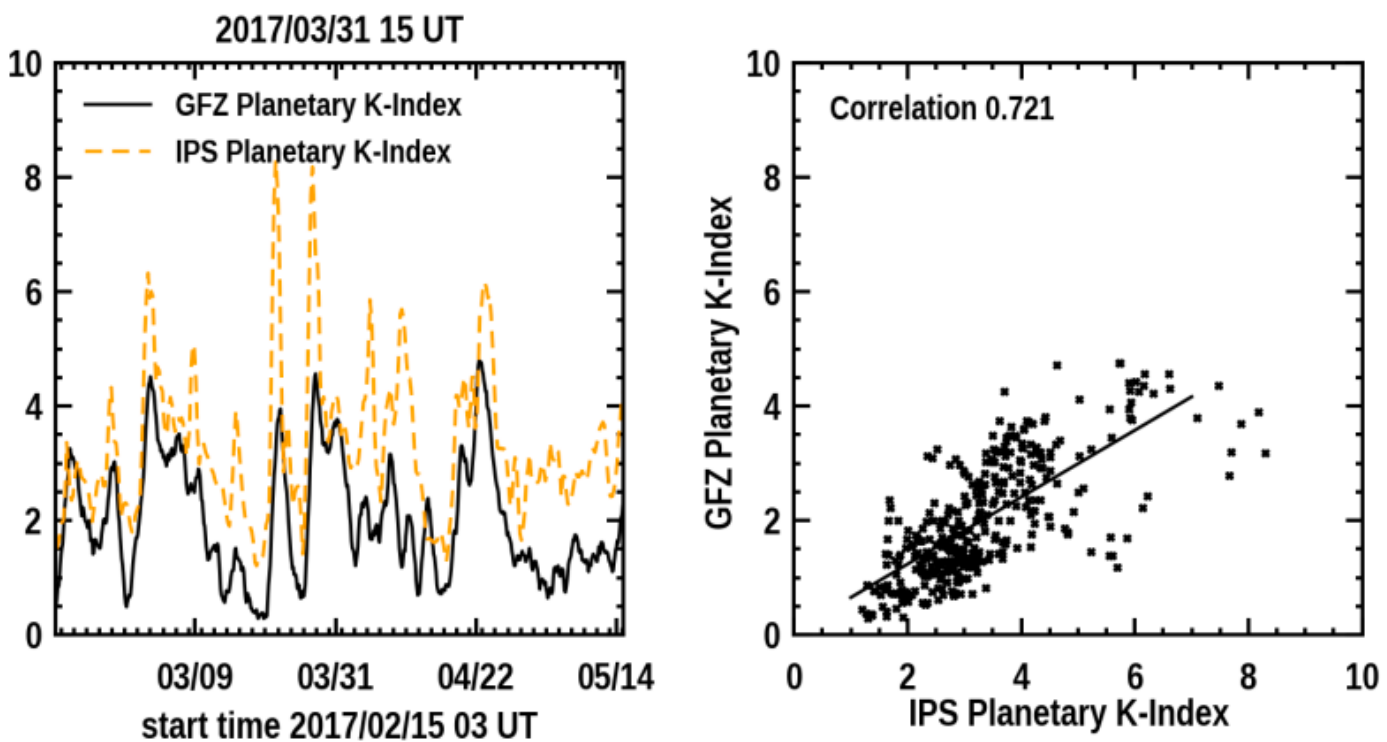
3. Kp Index from Machine Learning

The UCSD Kp machine learning tool we have developed uses not only a negative Bz forecast, but also the other two component fields as well as our UCSD forecast densities and velocities. These are currently available up to five days ahead of the program run time. From first principle comparative analyses (Newell *et al.*, 2007) we train the tool on the previous solar equinox period to match our low resolution values of Kp from velocity, density, and fields given by the tomography, and then test it with an adjustment match to the current amplitude and timing of our Kp values from past 14-day Kp measurements up to the future. Changes are made, if needed, to past Bz value timings. The schematic of how this works is shown below, as are the results for the -Bz excursion of Kp for 2024/04/20 (above). The analysis is updated every 6 hours as the forecast run time is closer to the forecast Kp increase; this enhances our ability to make better Kp forecasts.
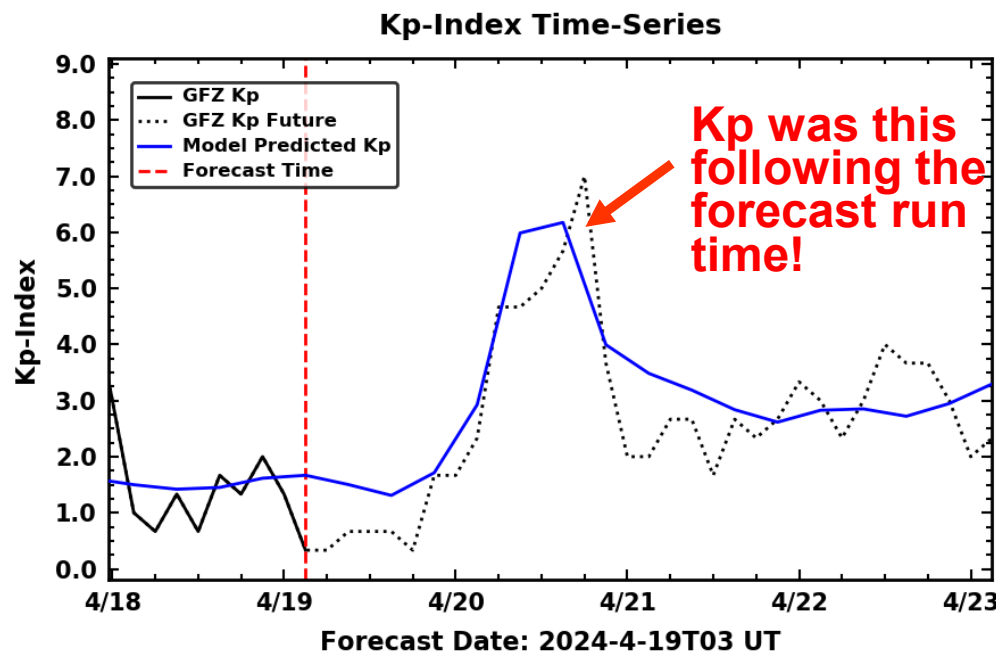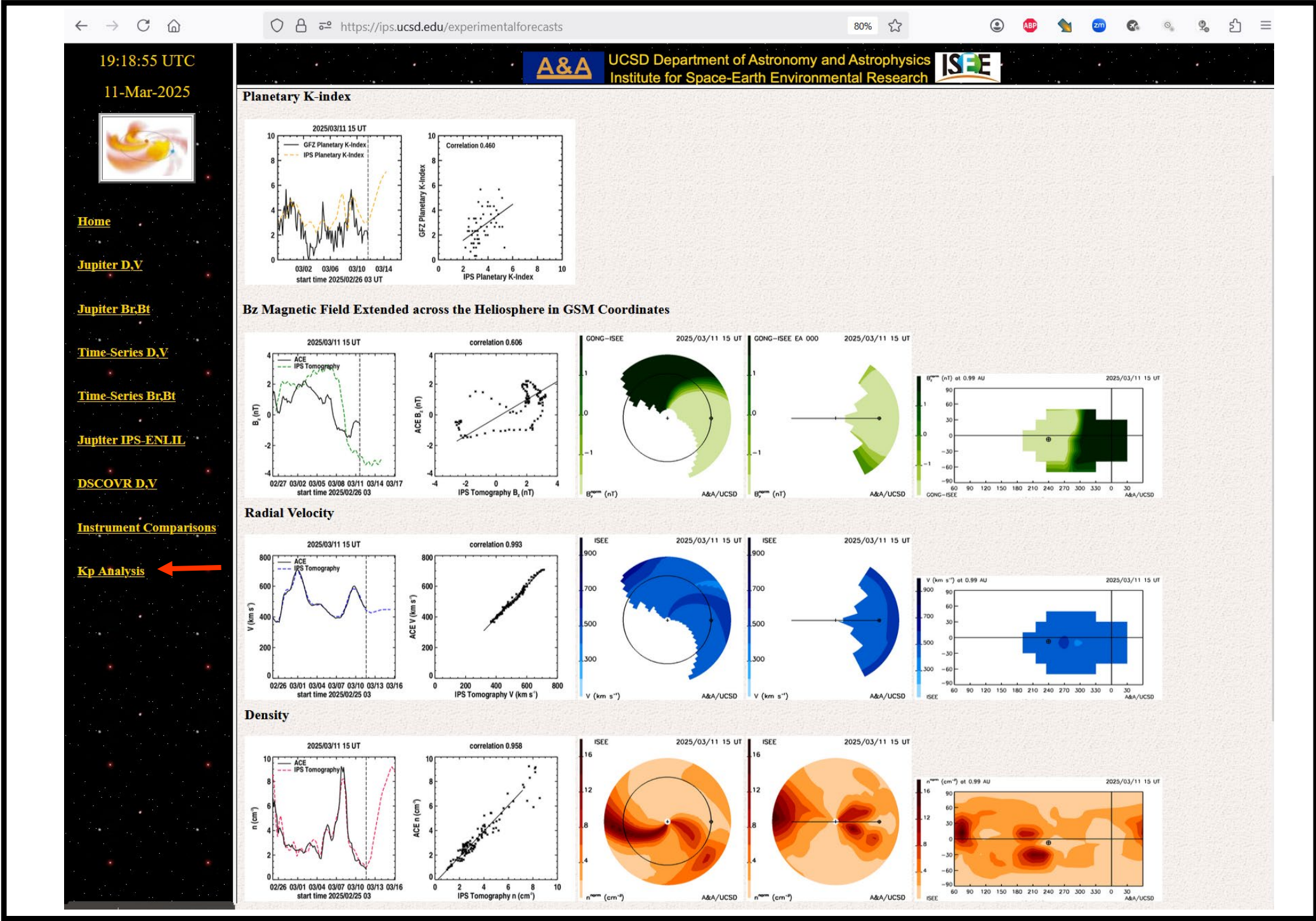
Kp training from the 2017 spring equinox.

Kp was this following the forecast run time!

Kp test case from the 2024/04/20 forecast

Kp Learning Procedure

(https://ips.ucsd.edu/experimentalforecasts)

Kp Analysis

Kp-Index Training Timeline

1. At the red points, determine a new best model with 4 months of data centered around each equinox. Produce 9 models with different time-shifts in magnetic field data. This occurs after Carlington rotation data from the e3 and Bxyz files are loaded in.
2. of these 9 models use the model with the best fit within the 14-day archive period used for each forecast (updates every 6 hours).
3. When it is time to train a new model, evaluate performance to determine re-training weights.

6-hour predictions
14-days   5 days
Archive   Forecast
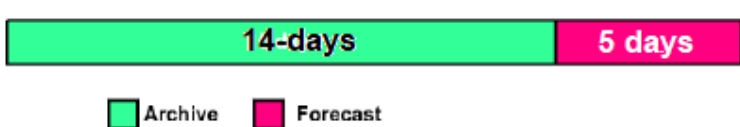
4. Real-Time Kp Forecast
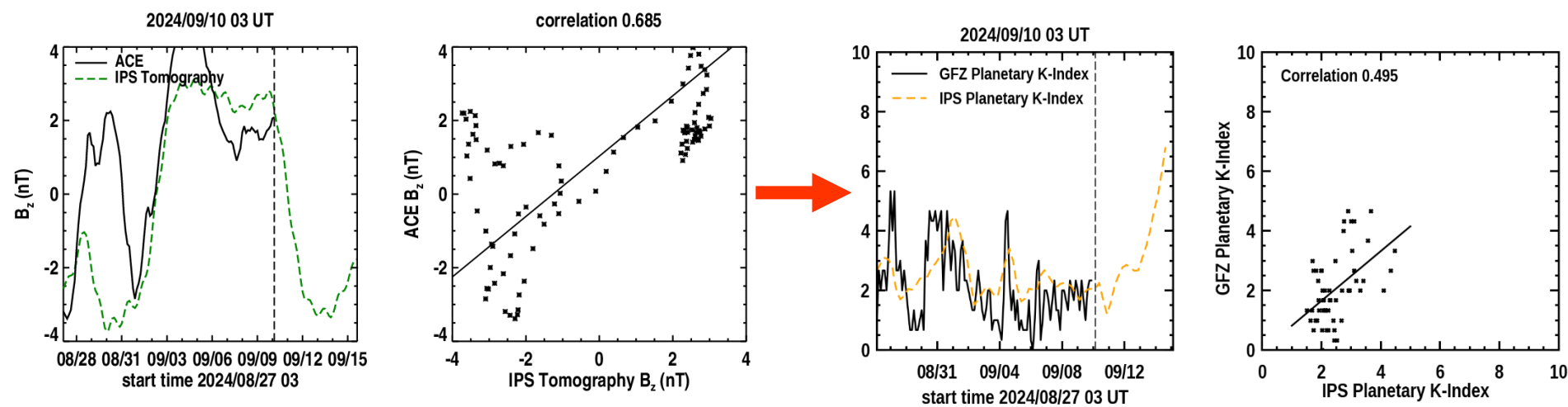
Kp test case from the 2024/09/17 forecast compared with Potsdam

Kp test case compared with Potsdam   **Still there after 4 days**

NOAA Kp

NOAA Kp

References:

Jackson, B.V., Hick, P.P., Buffington, A., Kojima, M., Tokumaru, M., Fujiki, K., Ohmi, T., and Yamashita, M.: 2003, Time-dependent tomography of heliospheric features using interplanetary scintillation (IPS) remote sensing observations, *CP679, Solar Wind Ten: Proceedings of the Tenth International Solar Wind Conference*, edited by M. Velli, R. Bruno, and F. Malara, pp75-78.

Jackson, B.V., Clover J.M., Hick, P.P., Buffington, A., Bisi, M.M., and Tokumaru, M.: 2013, Inclusion of Real-Time in-situ Measurements into the UCSD Time-Dependent Tomography and Its Use as a Forecast Algorithm, to TI: Heliosphere - Observation & Modeling, *Solar Phys.*, 285, 151-165, doi: 10.1007/s11207-012-0102-x.

Jackson, B.V., Buffington, A., Cota, L., Odstrcil, D., Bisi, M.M., Fallows, RF, and Tokumaru, M., 2020, 'Iterative Tomography: A Key to Providing Time-dependent 3-D Reconstructions of the Inner Heliosphere and the Unification of Space Weather Forecasting Techniques', *Frontiers in Astronomy and Space Sciences*, 19 pages, doi: 10.3389/fspas.2020.568429.

Jackson, B.V., Tokumaru, M., Fallows, R.A., Bisi, M.M., Fujiki, K., Chashei, I., Tyul'bashev, Chang, O., Barnes, D., Buffington, A, Cota, L., and Bracamontes, M.: 2022, Interplanetary Scintillation (IPS) analyses during LOFAR campaign mode periods that include the first three Parker Solar Probe close passes of the Sun, *Adv. Space Res.*, doi: 10.1016/j.asr.2022.06.029

Jackson, B.V., Tokumaru, M., Iwai, K., Bracamontes, M., Buffington, A., and Fujiki, K., Murakami, G., Heyner, D., Sanchez-Cano, B., Rojo, M., Aizawa, S., Andre, N., Barthe, A., Penou, E., Fedorov, A., Sauvaud, J.-A., Yokota, S., and Saito, Y., 2023, 'Forecasting heliospheric CME solar wind parameters using the UCSD time-dependent tomography and ISEE interplanetary scintillation data: the March10, 2022 CME', *Solar Phys.*, doi:10.1007 /s11207-023-02169-8.

Newell, P.T., Sotirelis, T., Meng, C.I., and Rich, F.J., 2007, 'A nearly universal solar wind-magnetosphere coupling function inferred from 10 magnetospheric state variables', *J. Geophys. Res.*, 112, A01206, doi: 10.1029/2006JA012015.

Parker, E.N.: 1958, 'Dynamics of the interplanetary gas and magnetic fields', *Astrophys. J.*, 128, 664-676.

Russell, C. T. & McPherron, R. L. (1973). Semiannual variation of geomagnetic activity, *J. Geophys. Res.*, 78, 92.

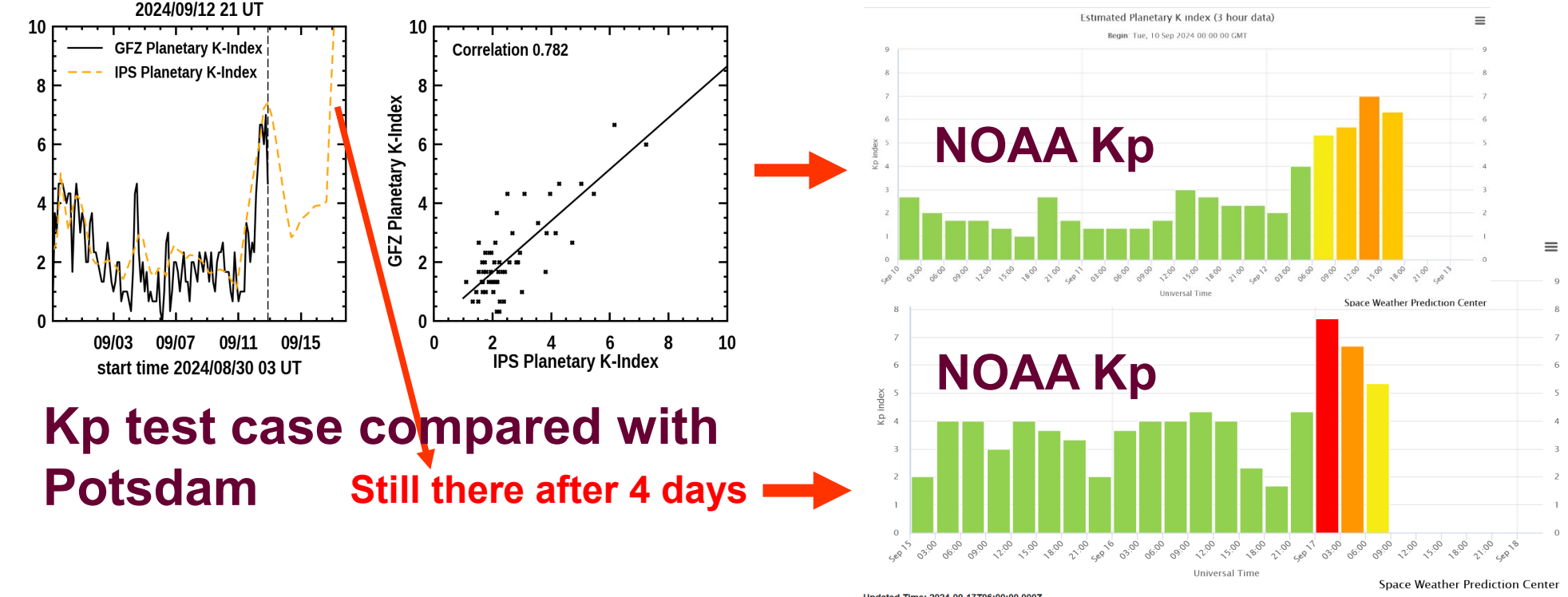Zhao, X., and Hoeksema, J.T.: 1995, Prediction of the interplanetary magnetic field strength, *J. Geophys. Res.*, 100, 19-33